PEG Nanocages as Non-sheddable Stabilizers for Drug Nanocrystals

Kathrin Fuhrmann, Jessica D. Schulz, Marc A. Gauthier, and Jean-Christophe Leroux*

Institute of Pharmaceutical Sciences, Department of Chemistry and Applied Biosciences, Swiss Federal Institute of Technology Zurich (ETH), Wolfgang-Pauli-Str. 10, 8093 Zurich, Switzerland

ABSTRACT

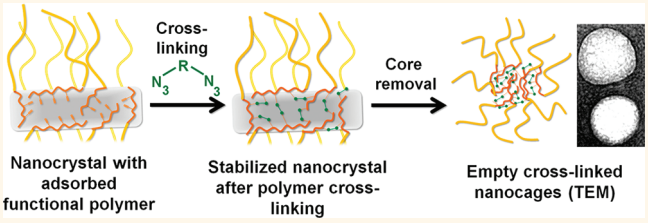

Many potent drugs are difficult to administer intravenously due to poor aqueous solubility. One validated approach for addressing this issue is to process them into colloidal dispersions known as "nanocrystals" (NCs). However, NCs possess high-energy surfaces that must be stabilized with surfactants to prevent aggregation. In addition, the stabilizer provides a means of anchoring targeting moieties to the NCs for achieving deposition or uptake at specified locations. Nevertheless, a critical challenge is that the surfactant (and consequently the targeting agents) can be shed upon high dilution. This work demonstrates successful cross-linking by click chemistry of stabilizers around paclitaxel NCs to form polymeric "nanocages". Cross-linking does not cause aggregation, as evidenced by transmission electron microscopy, and the nanocages retained the particulate drug through a combination of physical entrapment and physisorption. Size measurements by dynamic light scattering showed that nanocages act as sterically stabilizing barriers to particle—particle interactions and aggregation. The nanocages were shown to be less shed from the NCs than comparable non-cross-linked stabilizers. This contribution provides crucial general tools for preparing poorly sheddable stabilizing coatings to NCs and potentially other classes of nanoparticles for which covalent attachment of the stabilizer to the particle is undesirable (*e.g.*, a drug) or impossible (chemically inert). The presented approach also offers the possibility of more stably attaching targeting moieties to the latter by use of heterotelechelic PEG derivatives, which may favor active targeting and internalization by cells.

KEYWORDS: click chemistry · nanocrystals · polyester · biodegradable · paclitaxel · top-down process · ring-opening polymerization

Many modern and potent anticancer drugs are poorly water-soluble, which can create formulation problems when the drug is intended to be injected by the intravenous (i.v.) route.[1] Drug solubility may be altered on a number of levels including modification of the drug's structure (*e.g.*, change of crystalline form)[2] and by formulation approaches.[3] For example, paclitaxel (PTX), a potent antitumor agent, is typically formulated in a vehicle composed of polyethoxylated castor oil and dehydrated ethanol (Cremophor EL; Taxol).[4] However, owing to the required dose of Cremophor EL necessary to deliver a sufficient amount of PTX, a number of undesirable side effects have been observed.[5] In addition to the desire of eliminating large amounts of excipient, modern formulation strategies are also designed to increase the drug's therapeutic index by exploiting passive[6,7] and more recently active targeting. For instance, PTX has been formulated as a water-soluble prodrug,[8] as a polymer nanoconjugate,[9] conjugated to the natural lipid squalene,[10] in liposomes,[11] with carbon nanotubes,[12] as cyclodextrin complexes,[13] and in micelles.[14] Formulations that have been successfully applied or tested in the clinic are Abraxane, an albumin-bound nanoparticle system,[15] and Opaxio, a poly(L-glutamic acid)-based PTX conjugate (clinical phase III underway).[16] Nanosized systems have the potential to accumulate at cancer sites through the enhanced permeation and retention (EPR) effect and can possess targeting agents to promote active uptake by target cells or deposition at specific tumoral sites.

Current limitations include insufficient solubilization capacity,[17] potential excipient-related toxicity,[5,18] instability upon dilution in the bloodstream,[19,20] manufacturing difficulties, and drug stability issues during processing.[21] One validated and robust approach for addressing these issues is to process the drug powder into colloidal dispersions known as "nanocrystals" (NCs).[22−25] Wet milling can produce uniformly sized drug NCs with mean diameters of less than 200 nm and little batch-to-batch variability.[26] This top-down process is suitable for many different classes of compounds, and there currently exist several oral formulations produced by wet milling

* Address correspondence to jleroux@ethz.ch.

Received for review November 30, 2011 and accepted February 1, 2012.

Published online February 01, 2012
10.1021/nn2046554

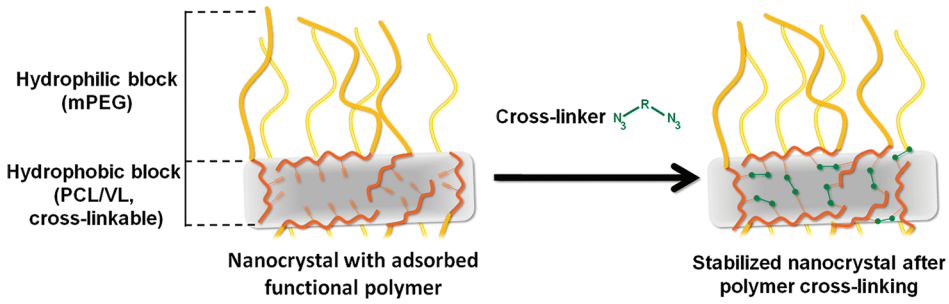

Figure 1. Schematic representation of diblock copolymer self-assembly on the surface of drug NCs and nanocage formation following cross-linking.

on the market.[27] One key feature of NCs is the minimal use of excipients compared to other formulation approaches, which implies both high drug content and diminished excipient-related toxicity. For the i.v. route, NCs are promising drug carriers because their very high loading can lead to higher deposition of drug in cancer cells upon delivery.[28] Indeed, there is increasing evidence that drug NCs can accumulate in tumors *via* the EPR effect.[29]

NCs are generally stabilized with surfactants (or "stabilizers"), whose functional role is to prevent aggregation between the high-energy crystal surfaces produced during the size-reduction process. Consequently, much research is now directed toward optimizing the coating.[30] For example, Agarwal *et al.* have produced stable NCs of hydrophobic drugs by sonication and layer-by-layer assembly of oppositely charged polyelectrolytes leading to electrostatic repulsion between NCs.[31] Similarly, Abraxane is an injectable NC formulation of PTX produced by high-pressure homogenization in the presence of human serum albumin, which acts as a steric stabilizer for the NCs.[32] In addition, the stabilizer provides a means of anchoring targeting moieties to the NCs. For example, Liu *et al.* have modified poloxamer 407 with folic acid and have shown enhanced cellular uptake of targeted PTX NCs, in comparison to untargeted ones.[28] A recent study by Sugahara *et al.* has investigated the efficacy of PTX NCs when co-administered with a tumor-penetrating peptide and of Abraxane decorated with the latter.[33] The authors have shown that these approaches could slightly enhance the antitumoral effect.[34] However, a critical challenge in achieving active targeting is the possibility that the targeting agents are shed along with the stabilizer upon high dilution. For instance, Deng *et al.* have indirectly shown that poloxamer 407 can desorb from PTX NCs upon mild heating or dilution.[35] The authors also found that the conditions under which the NCs are prepared can lead to different affinities between the polymer and the drug.

The objective of this study was to prepare non- or poorly sheddable biodegradable stabilizers for NCs that are maintained in place independently of specific stabilizer–drug interactions. It was hypothesized that this could be accomplished by chemical cross-linking of the stabilizer around the NC, thereby maintaining the drug in place by a combination of physical entrapment and physisorption. Conceptually, the cross-linked polymer coating forms a polymeric "nanocage" in which the NC is trapped. Earlier work on nanocages has been reported by Turner *et al.*[36] These were prepared in a multistep process involving shell cross-linking of micellar structures, core digestion, and functionalization with lipids to improve subsequent drug loading. In contrast to their method, the specific challenge addressed herein lies in performing cross-linking reactions near the surface of PTX NCs, due to the presence of high-reactive crystal surfaces and to reactions taking place in a heterogeneous phase. As illustrated in Figure 1, herein is reported the preparation of PTX NCs by wet milling with amphiphilic biodegradable and cross-linkable copolymers and conditions for successfully cross-linking them to form a nanocage–NC construct. Evidence for the lower sheddability of the nanocage in comparison to non-cross-linked stabilizers is given. This approach is advantageous because it can easily be adapted to the grafting of targeting ligands. In addition, as the stabilizing coating is maintained in place more or less independently of specific drug–polymer interactions, it should be amenable to other hydrophobic drugs.

RESULTS AND DISCUSSION

Polymer Design and Synthesis. A number of differing polymeric agents have been examined as steric stabilizers for drug NCs. The currently used systems are maintained on the surface of NCs through physisorption,[25,35] an equilibrium process which can lead to the reversible desorption of the stabilizer upon dilution or heating.[35] To examine the hypothesis that a non-sheddable stabilizing nanocage can be made, a cross-linkable amphiphilic polymer was prepared. The structure of the stabilizers and cross-linking agents examined in this study are illustrated in Scheme 1. The stabilizing copolymer was designed to contain mPEG as the hydrophilic polymer segment to act as a steric stabilizing agent for the NCs and thereby prevent NC agglomeration by masking their high-energy surfaces.

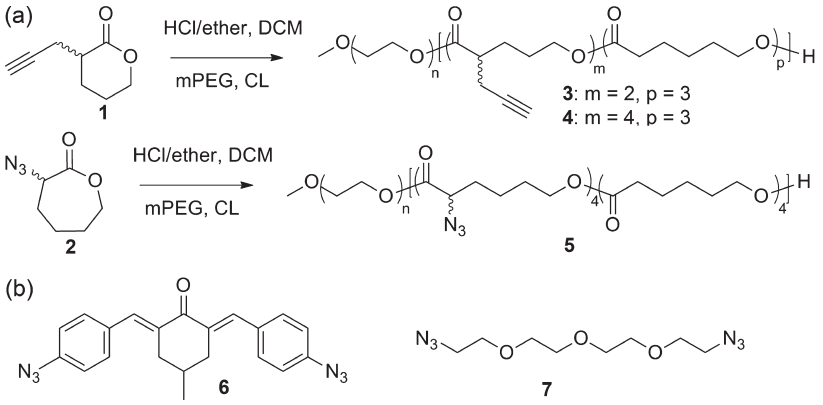

Scheme 1. (a) Synthesis of polymers 3, 4, and 5 from functional monomers 1 or 2 and ε-caprolactone (CL) from an mPEG macroinitiator; (b) structure of small molecule cross-linking agents 2,6-bis(4-azidobenzylidene)-4-methylcyclohexanone (6) and 1,11-diazido-3,6,9-trioxaundecane (7).

In addition, this polymer should decrease opsonization and convey "stealth-like" properties to the NCs.[1,37,38] Also, a variety of heterotelechelic variants of this polymer are commercially available, which opens the opportunity for future functionalization of the hydrophilic corona of stabilized NCs. Poly(ε-caprolactone) was selected in favor of other polyesters because of its hydrophobicity and slow degradability.[39] It was rationalized that these properties would minimize polymer degradation during the milling process and favor the hydrophobic interactions with the drug NC. In addition, there are medical devices fabricated with poly(ε-caprolactone) which have FDA approval (suture materials like coated Monoderm or Monocryl (poliglecaprone 25)). The hydrophobic block was prepared by statistical cationic ring-opening copolymerization (ROP) of ε-caprolactone with functional lactone monomers.[40] A short hydrophobic segment was selected (*ca.* 5−7 units) so that the overall strength of the interaction between the polymer and the drug was moderate to low. As a consequence, findings obtained using this polymer may be relatively independent of specifically strong (or weak) polymer−drug interactions. Several recent reports have investigated other ROP approaches for preparing functional polyesters.[41,42] Cationic ROP is advantageous for producing polymers for pharmaceutical applications owing to the absence of commonly used tin-containing catalysts.[41] ε-Caprolactone was copolymerized with variable ratios of **1** to produce **3** and **4**. These polymers had monomodal and narrow molecular weight distributions (Supporting Information Figure S1) and contained on average two and four alkynyl groups per polymer chain for **3** and **4**, respectively, as determined by ^{1}H NMR spectroscopy (Supporting Information Figures S2 and S3). An azido analogue of **3** and **4** was prepared in the same fashion as above by replacing **1** with **2** in the polymerization reaction. The resulting polymer, **5**, also had a narrow and monomodal molecular weight distribution and contained on average four azido units per polymer (Supporting Information Figures S1 and S4). Precipitation with ether or hexane was sufficient for removing unreacted monomer and hydrophobic oligomers not connected to mPEG (*i.e.*, initiated by trace water in the reaction vessel) as evidenced by analytical SEC (Supporting Information Figure S1).

Preparation of Cross-Linkable NCs. PTX was milled in the presence of **3** and the size reduction monitored with time (Supporting Information Figure S5). A stable and reproducible particle size of about 200 nm was achievable by milling for 48 h, which was the smallest size achievable with the current experimental setup. This time was substantially shorter than the seven days reported for poloxamer 407,[43] with similar milling equipment. The size and shape of particles obtained were consistent with values reported for paclitaxel and other drug NCs produced by wet milling.[43−45] The characteristic needle-like structure of paclitaxel NCs was always observed using this process (Figure 2A,B). Owing to their similarity, comparable particle sizes were obtained using **3** and **4**. Briefly centrifuging the crude suspension of NCs to remove larger aggregates had only a small effect on mean particle size and polydispersity (Supporting Information Figure S6) confirming a narrow distribution of particle sizes. The suspensions were purified from excess polymer by SEC, yielding a suspension with a typical concentration of 0.55 or 0.74 mg/mL PTX when using **3** or **4**, respectively. The recovered yields depended on the initial particle size after milling and the centrifugation step, which removed less drug in case of the smaller particles. Owing to the biodegradable nature of the hydrophobic block, the stability of the polymer during the milling process was assessed by analytical SEC. In a drug-free run, a slight decrease of polymer molecular weight was observed after 96 h of milling, which is twice as long as the time used for NC preparation (Supporting Information Figure S7).

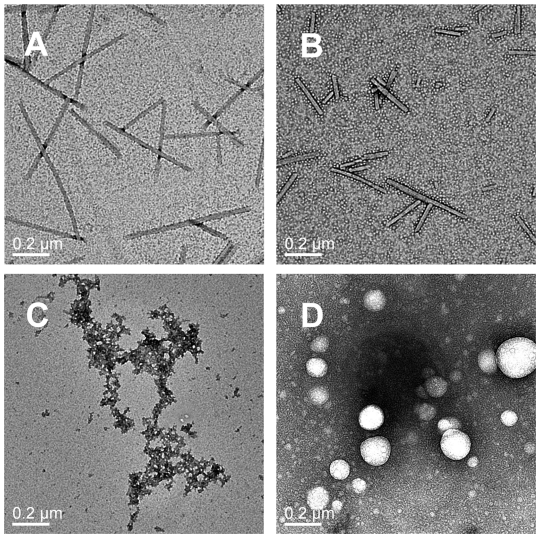

Figure 2. TEM images of NCs stabilized with 3 before (A) and after cross-linking (B) with 7 (2.5/1 azide/alkyne). Following dissolution of the NCs from A and B in 25% ethanol, an aggregate structure was observed for the non-cross-linked NCs (C) while intact polymeric coatings were observed for the correspondingly cross-linked NCs, in the form of discrete spheroids (D).

TABLE 1. Conditions of Cross-Linking Experiments

polymer (mM)	cross-linker	azide/alkyne molar ratio	$CuSO_4$ (mM)	ascorbate (mM)	time (h)
in solution					
3 (1.8)	**7**	1/1	1.8	9	0.3
3 (1.8)	**7**	1/10			
on NCs					
3 (0.087)	**7**	2.5/1	0.067	0.333	24
3 (0.087)	**7**	10/1			
3 (0.087)	**7**	15/1			
4 (0.114)	**5**	2/1			
4 (0.114)	**6**	2/1			
4 (0.114)	**7**	15/1			

To quantify the amount of polymer per drug NC, ^{1}H NMR spectra of the NCs stabilized with **3** and **4** were recorded in $CDCl_3$, a good solvent for both polymer and drug (Supporting Information Figure S8). By comparing the signals from the aromatic protons of PTX (8.12 ppm) and the signal of PEG (3.64 ppm), a molar polymer/drug ratio of 0.134:1 (approximately 1:2 w/w) was obtained. Thus the drug content of the PTX NCs was approximately 67 wt %, a value which is comparable or higher to that reported for other drug/stabilizer systems.[35,43] Drug content was comparable when either **3** or **4** were used as stabilizers. TEM analysis of the stabilized NCs showed the characteristic needle-like shape of PTX and lack of aggregation (Figure 2A,B). From these and additional images, the average length and diameter of the NCs were 206 × 26 nm (n = 138), respectively. Considering the weight ratio of polymer

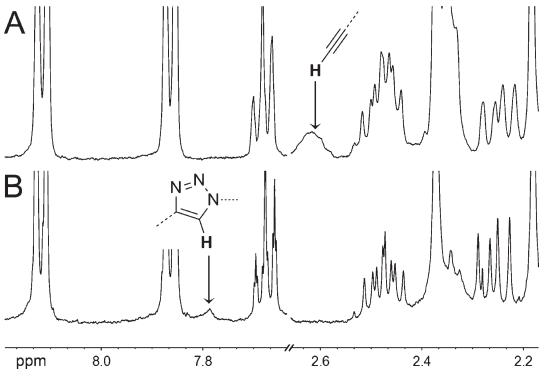

Figure 3. ^{1}H NMR spectra of NCs stabilized with 3 before (A) and after (B) cross-linking with 7 (azide/alkyne ratio 10/1). Signals belonging to the acetylene proton at 2.59 ppm were reduced, and a peak for the resulting triazole at 7.78 ppm appeared. A break on the *x*-axis between 7.6 and 2.7 ppm was added for clarity.

to drug, and assuming the drug NCs to be cylinders, one can estimate that approximately 1.35 × 10^4 polymer chains are adsorbed per NC. This equates to 1.34 nm^2/polymer chain or an ethylene glycol monomer density of 34/nm^2, which both point to the polymer adopting a brush-like conformation.[46,47] This type of conformation is advantageous for preventing clearance by the mononuclear phagocyte system.

Cross-Linking and Purification of Cross-Linked NCs. *General Considerations.* In a proof of principle experiment, **3** was cross-linked with **7** in solution and in the absence of NCs (Table 1). The reaction was monitored by ^{1}H NMR and FTIR spectroscopy to verify the consumption of alkynyl and azido peaks and the appearance of the triazole product (Supporting Information Figures S9 and S10). At a stoichiometric azide to alkyne ratio, both reacting groups were completely consumed within 20 min, indicating that the alkynyl groups on **3** were readily available for reaction in the absence of NCs.

In general, for cross-linking the NCs, a lower concentration of copper sulfate and sodium ascorbate was used compared to the reaction in solution above because insoluble copper(I) salts caused rapid destabilization and aggregation of the NCs. Cross-linking performed at 6 °C also resulted in the formation of large aggregates, indicating that the reaction should be carried out at room temperature. An optimal cross-linking time of 24 h was found for the NCs (no further evolution of their ^{1}H NMR spectra after this reaction duration). After the reaction, the salts were removed from the cross-linked NCs by SEC. For this purpose, Sephadex G10 had to be employed because the interactions between cross-linked NCs and Sepharose CL-4B lead to column blockage or very low recovery of the NCs. Inductively coupled plasma optical emission spectroscopy (ICP-OES) analysis revealed less than 1 ppm residual copper after purification. This result could be improved by increasing the column length or by performing a second purification by SEC.

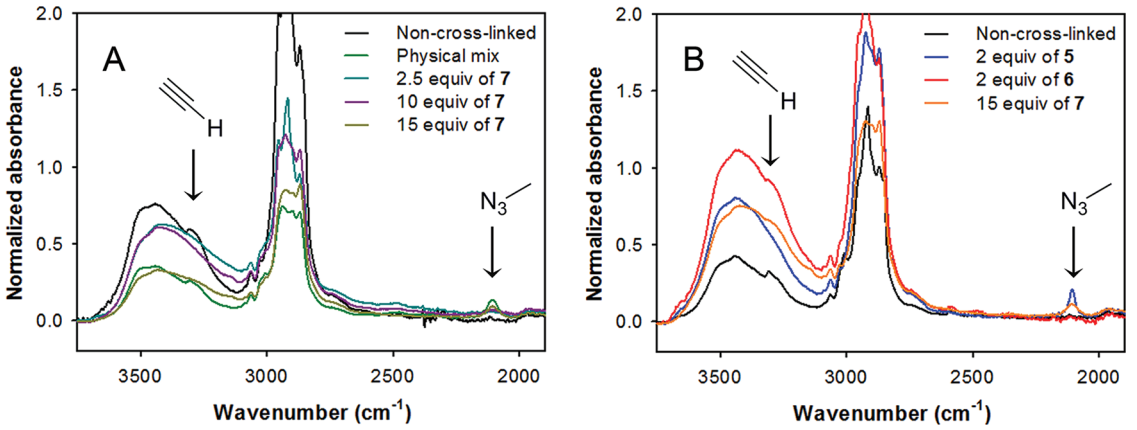

Figure 4. FTIR spectra of NCs stabilized with 3 (A) or 4 (B) before cross-linking, in a physical mix with 7, and following cross-linking. After cross-linking, signals from the alkyne decreased or disappeared, while the azide band completely disappeared, providing a strong indication of cross-linking. Only for the NCs cross-linked with 5 was residual azide observed, possibly due to lower reactivity of the polymeric tetra-azide.

Analysis of the Extent of Cross-Linking. Following purification, analysis of the extent of cross-linking was complicated by reduced possibilities for dissolving the nanocage. For instance, after reaction with excess **7** (10/1 azide/alkyne), purification, and lyophilization, the NCs were no longer fully soluble in chloroform, indicating successful interpolymer chain cross-linking. Sonication of the cross-linked polymer coating while heating in deuterated methanol lead to a homogeneous suspension which could be analyzed by ^{1}H NMR spectroscopy (Figure 3). From this spectrum, a decrease of the intensity of the alkynyl protons and the appearance of a peak for the triazole groups could be observed, though both were slightly shifted in comparison to those observed for the polymers in solution, which were analyzed in deuterated chloroform. Quantitative disappearance of the alkynyl group (2.59 ppm) was observed for **3** when cross-linked with 10 equiv or more of **7**. FTIR spectroscopy of the NCs before and after cross-linking also qualitatively revealed the decrease of the band associated with the alkynyl group (3270 cm^{-1}), indicating reaction (Figure 4A). The absence of the band for the azido group (2100 cm^{-1}) indicated both successful removal of excess diazido reagent during the purification step and argues in favor of bivalent reaction of **7** with the polymer (*i.e.*, reaction of both rather than a single azide of **7** with the alkynyl groups). In contrast, NCs prepared with **4** had lower conversion of the alkynyl group (85, 65, and 75% for **5**, **6**, and **7**, respectively) and showed residual azide by FTIR spectroscopy (Figure 4B). As evidenced by TEM (Figure 2B), inter-NC cross-linking was not observed.

To verify that the polymer coating was indeed cross-linked, NCs were dialyzed against an ethanol/water mixture to remove the drug from the polymer network. The dialysis membrane was selected so that the polymer and dissolved drug molecules could freely pass through the pores, while the cross-linked polymer, because of its higher molecular weight, remained trapped inside. Following reaction with CoSCN, residual mPEG was detected in the dialysis bag containing the cross-linked NCs, while none was detected for the non-cross-linked analogues (Supporting Information Figure S11). TEM imaging revealed the presence of intact polymeric spheroids for the cross-linked samples (Figure 2D), proof for intermolecular cross-linking, but showed dense aggregates, probably residual polyester, for the non-cross-linked analogues (Figure 2C). These experiments demonstrated that the nanocage remained structurally intact even following complete removal of the drug. Although different, this system is reminiscent of hollow cage-like structures, as prepared by Turner and Wooley, which were obtained after core degradation of shell cross-linked particles.[48]

Sheddability of the Polymer Nanocages. Owing to its adequate water solubility, the influence of cross-linking excess on particle size stability was examined using **7** and NCs stabilized with **3**. Azide/alkyne ratios of 2.5/1, 10/1, and 15/1 were examined, as listed in Table 1. NCs stored at 6 °C showed very little or no change of size over a period of three weeks (Supporting Information Figure S12), which was comparable to findings from the literature.[44] At room temperature, an increase of particle size with time was observed for all samples. As seen in Figure 5, cross-linking led to enhanced size stability in comparison to NCs with non-cross-linked stabilizers. Owing to the relatively short hydrophobic anchoring moieties on **3** and **4**, strong interaction between these and the PTX NCs is unlikely. Consequently, while the cross-linked coating is likely to prevent NC growth by aggregation, it may not efficiently prevent crystal growth by Ostwald ripening.[49,50] This is consistent with the lack of crystal growth at 6 °C (Supporting Information Figure S12), where the solubility of PTX is lower than at 20 °C, thereby slowing ripening. Future experiments involving more polymer layers, longer hydrophobic segments and/or hydrophobic segments capable of

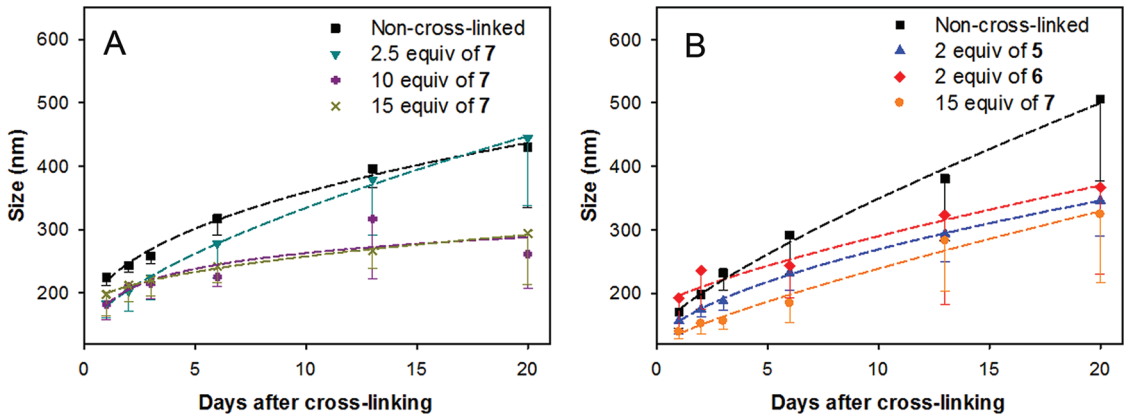

Figure 5. Evolution of NC size over time. (A) Non-cross-linked and cross-linked NCs stabilized with 3 and cross-linked with 7. On day 6, the size of non-cross-linked NCs was significantly different from those cross-linked with 10 and 15 equiv of 7 ($p < 0.05$; $n = 6$). (B) Non-cross-linked and cross-linked NCs stabilized with 4 and cross-linked with 5−7. On days 3, 6, and 20, the size of non-cross-linked NC was significantly different from those which were cross-linked with 5 and 7; on day 13, only non-cross-linked and cross-linked with 7 were different ($p < 0.05$; $n = 6 - 13$). Values represent means − SD.

tightly packing on the surface of the NC may provide insight as to whether the nanocages can fully prevent Ostwald ripening. For now, storage at 6 °C was found to be sufficient for preventing this process.

It was observed that the size stability of the cross-linked NCs improved with increased feed azide/alkyne ratios up to 10/1, at which point differences were no longer observed. This indicated that maximal conversion of the alkynyl group was achieved at this ratio. Overall, these results indicated that cross-linking is an important parameter in slowing crystal growth and argued in favor of nanocage desorption being reduced in comparison to the non-cross-linked control. Increasing the number of alkynyl groups on the polymer (*i.e.*, NCs stabilized with **4**, bearing four cross-linkable groups per chain) did not influence the results significantly in comparison to those obtained with **3** (Figure 5B).

The relative sheddability of the polymer coatings before and after cross-linking was analyzed by quantifying by ^{1}H NMR the amount of dissolved mPEG present in the supernatant of freshly centrifuged NC dispersions (Supporting Information Figure S13). In comparison to non-cross-linked NCs, the cross-linked analogues showed between 3−4-fold less mPEG in the supernatant, as determined for two different batches of NCs. This experiment demonstrated that cross-linking the surfactant to form a nanocage favors retention of the latter on the surface of the NC.

NC−nanocage Interactions. Two additional cross-linking agents were selected based on their different physicochemical characteristics, which could potentially influence the nature of the interactions between the polymer nanocages and the NCs. **5** is a polymeric cross-linking agent with a structure analogous to **3** and **4**, but with four azido groups in its hydrophobic segment. These could promote greater interchain cross-linking. However, owing to its amphiphilic nature, it was only added in small amounts as competition with **4** for the surface of the NC prior to cross-linking was anticipated. **5** displayed a similar stabilizing effect to **7**, though with less cross-linker added. In addition, the FTIR spectrum of these NCs revealed the presence of residual azido groups, indicating incomplete conversion of these groups on the NCs. **6** is a hydrophobic cross-linking agent that should preferentially partition to the surface of NCs, thereby not only favoring cross-linking but also interaction between the hydrophobic segments of the nanocage and the NC. However, only low concentrations could be used since the compound, owing to its poor water solubility, precipitated from its organic solution upon mixing with water. When the nature of the cross-linking agent was altered to more hydrophobic **6**, no statistical difference in size was observed in comparison to the non-cross-linked NCs (Figure 5B). These results indicate that specific drug−nanocage interactions do not play a large role on size stability of the NCs at least within the range of modifications examined (*i.e.*, two hydrophobic anchoring groups and three cross-linking agents). Due to its unknown toxicity and small molecular weight, this compound was uniquely used for gaining a better understanding of the nanocage system and was not intended for *in vivo* use.

Drug Dissolution under Sink Conditions. NCs of PTX have previously been shown to possess sufficiently long circulation times to benefit from passive accumulation in tumors.[28,51] The dissolution kinetics of the NCs were evaluated herein under sink conditions to assess whether the lack of desorption of the polymer nanocage was an influencial factor on the latter. The dissolution characteristics of all NCs, cross-linked and non-cross-linked, were overall statistically the same (Supporting Information Figure S14). Under the present experimental conditions, the polymer nanocage was expected to remain intact over the entire time

frame of the experiment and maintain residual drug particle within its hydrophobic core due to a combination of physical entrapment and physisorption. From these results, it was found that about 50% of the NCs dissolved in more than 3 h. This time frame would be sufficient for high deposition of drug in the tumor tissue if a targeting ligand were attached to the nanocage.[33] In addition to the high surface coverage with mPEG, the high aspect ratio of the NCs (Figure 2A,B) might increase circulation time, as has been observed in other studies.[52]

CONCLUSION

This work demonstrated successful cross-linking of polymeric stabilizers around PTX NCs to form polymeric nanocages. These retained the particulate drug through a combination of physical entrapment and physisorption. The nanocages were found to act as sterically stabilizing barriers to particle−particle interactions and aggregation. These were also shown to be shed to a lesser extent than non-cross-linked coatings, thereby providing a means for enhanced retention of targeting agents on NCs. These findings provide crucial tools for preparing non-sheddable stabilizing coatings for NCs and potentially other classes of nanoparticles under circumstances where covalent attachment between the coating and the particle is not possible or desired. In addition, the proposed strategy should be applicable to other polyesters to thereby modulate the rate of degradation of the nanocage. In theory, it should be possible to attach targeting ligands to the nanocage by use of heterotelechelic PEG derivatives and thus access active targeting or internalization of NCs.

METHODS

Materials. PTX was obtained from Bioxel Pharma Inc. (Sainte-Foy, QC, Canada) and docetaxel from ScinoPharm Taiwan, Ltd. (Tainan County, Taiwan). Sepharose CL-4B, Sephadex G10, lithium diisopropylamide (LDA), δ-valerolactone, propargyl bromide, hexamethylphosphoramide (HMPA), ε-caprolactone, 2, 6-bis(4-azidobenzylidene)-4-methylcyclohexanone (97%, containing 35−45% water), sodium azide, copper(II) sulfate, albumin from bovine serum (BSA; ≥96%), and methoxy poly(ethylene glycol) (mPEG; 2000 g/mol) were purchased from Sigma-Aldrich (Buchs, Switzerland) and used as received. Hydrogen chloride (1 N solution in diethyl ether), *m*-chloroperoxybenzoic acid (*m*CPBA, 70−75%), and 1-methyl-2-pyrrolidinone were purchased from Chemie Brunschwig AG (Basel, Switzerland). 1,11-Diazido-3,6,9-trioxaundecane was obtained from Santa Cruz Biotechnology (Santa Cruz, CA), sodium L-(+)-ascorbate from Axon Lab AG (Baden-Dättwil, Switzerland), and deuterium oxide from ReseaChem GmbH (Burgdorf, Switzerland). Ultrapure water was prepared by a Barnstead Nanopure system (Thermo Fisher Scientific, Reinach, Switzerland). Dry solvents were taken from a solvent purification system (LC Technology Solutions Inc., Seabrook, NH). δ-Valerolactone and ε-caprolactone were distilled over calcium hydride under inert atmosphere before use. All other solvents were of highest purity and bought from Sigma-Aldrich (Buchs, Switzerland).

Synthesis of α-Propargyl-δ-valerolactone (1). The synthesis of **1** was adapted from Parrish *et al.*[41] LDA (6.49 mL, 11.69 mmol, 1.1 equiv) was dissolved in THF and cooled to −78 °C. A solution of δ-valerolactone (0.96 mL, 10.63 mmol, 1 equiv) in THF was added dropwise over 1 h and then stirred for another 30 min. Propargyl bromide (1.14 mL, 12.75 mmol, 1.2 equiv) and HMPA (2.22 mL, 12.75 mmol, 1.2 equiv) were added dropwise over 10 min. The brown reaction mixture was warmed to approximately −42 °C, and the temperature was maintained while stirring for 3 h. After this period, 2.5 mL of a saturated solution of ammonium chloride was added, and the reaction was allowed to warm to room temperature. Volatiles were removed by rotary evaporation, and the residual yellow oil was dissolved in diethyl ether (40 mL), which was washed three times with brine (40 mL). The organic phase was dried over $MgSO_4$ and concentrated by rotary evaporation. After column chromatography (30% ethyl acetate in hexane, R_f 0.35) and distillation under reduced pressure (160 °C, 10 mbar), a colorless viscous liquid was obtained (0.675 g, 4.9 mmol, 46% yield). The density of **1** was measured by weighing pipetted volumes (n = 10) and determined to be 1.10 g/mL: ^{1}H NMR (400 MHz, $CDCl_3$, δ) 4.37−4.27 (m, 2H, CH_2O), 2.74−2.61 (m, 2H, $COCHCH_2C{\equiv}C$), 2.53−2.46 (m, 1H, $COCHCH_2$), 2.33−2.24 (m, 1H, $CHCH_2CH_2$), 2.01 (t, J = 2.6 Hz, 1H, $C{\equiv}CH$), 1.98−1.87 (m, 2H, $OCH_2CH_2CH_2$), 1.77−1.67 (m, 1H, $COCHCH_2CH_2$) (for an annotated spectrum, see Supporting Information Figure S15).

Synthesis of α-Azido-ε-caprolactone (2). The first step of the synthesis of **2** was adapted from Lenoir *et al.*[53] 2-Chlorocyclohexanone (1.98 g, 15 mmol, 1 equiv) was dissolved in 20 mL of dichloromethane to which *m*CPBA (4.1 g, 16.5 mmol, 1.1 equiv) was added. The reaction was stirred for 96 h at room temperature then stopped by cooling to −20 °C for 1 h. The precipitated *m*CPBA was removed by filtration to yield a pale viscous liquid, which was purified by column chromatography (35% ethyl acetate in hexane, R_f 0.32) to yield α-chloro-ε-caprolactone (1.033 g, 7 mmol, 45% yield): ^{1}H NMR (400 MHz, $CDCl_3$, δ) 4.80 (dd, J = 7.9, 2.7 Hz, 1H, $COCHCl$), 4.63 (ddd, J = 12.8, 7.8, 1.8 Hz, 1H CH_2CH_2O), 4.23 (ddd, J = 12.7, 7.4, 1.8 Hz, 1H, CH_2CH_2O), 2.23−1.77 (m, 6H, $ClCHCH_2CH_2CH_2$) (^{1}H NMR spectrum in Supporting Information Figure S16). In a second step, α-chloro-ε-caprolactone (500 mg, 3.4 mmol, 1 equiv) was added to a solution of sodium azide (1.1 g, 16.9 mmol, 5 equiv) in DMSO (30 mL) and stirred at 50 °C for 48 h. The turbid yellow mixture was diluted with water (150 mL) and extracted three times against 50% ethyl acetate in hexane (40 mL). The organic phases were combined, dried over sodium sulfate, and concentrated by rotary evaporation under reduced pressure to yield **2** as a viscous pale liquid (0.299 g, 1.9 mmol, 60% yield): ^{1}H NMR (400 MHz, $CDCl_3$, δ) 4.45−4.40 (m, 1H, $COCHN_3$), 4.18−4.12 (m, 2H, CH_2CH_2O), 2.09−1.67 (m, 6H, $N_3CHCH_2CH_2CH_2$) (Supporting Information Figure S17). The density of **2** (1.154 g/mL) was measured by weighing pipetted volumes (n = 6).

General Polymerization Procedure and Synthesis of mPEG-*b*-(εCL-*co*-1) (3). The polymerization procedure was adapted from Kim *et al.*[40] In a typical experiment, mPEG (800 mg, 0.4 mmol, 1 equiv) was dried by azeotropic distillation with dry toluene (50 mL) under a flow of nitrogen. The flask was sealed, and the mPEG was dissolved in dry dichloromethane (2 mL). Dry ε-caprolactone (132.8 μL, 1.2 mmol, 3 equiv) and **1** (150.5 μL, 1.2 mmol, 3 equiv) were then added using gastight syringes. The polymerization was initiated by the addition of HCl in ether (1.2 mL, 1.2 mmol, 3 equiv) and stirred at room temperature for 24 h. The reaction mixture was then precipitated twice in cold ether, the solvent evaporated *in vacuo*, the residue taken up in water, and the polymer recovered by lyophilization (0.867 g, 80% yield). The fully annotated NMR spectrum of **3** can be found in Supporting Information Figure S2. This polymer contained on average two

units of **1** per polymer chain. SEC (DMF): M_n = 2200 g/mol, M_w/M_n = 1.11.

Synthesis of mPEG-*b*-(εCL-*co*-1) (4). According to the general procedure described above, mPEG (1.50 g, 0.75 mmol, 1 equiv) was dried by azeotropic distillation with toluene and dissolved in dry dichloromethane. Then, dry ε-caprolactone (166 μL, 1.5 mmol, 2 equiv) and **1** (376.4 μL, 3 mmol, 4 equiv) were introduced, and the polymerization was started by the addition of HCl in ether (1.5 mL, 1.5 mmol, 2 equiv). After 24 h, the polymer was precipitated with diethyl ether, affording **4** as a white solid. The fully annotated NMR spectrum can be found in Supporting Information Figure S3. This polymer contains on average four units of **1** per polymer chain. SEC (DMF): M_n = 2700 g/mol, M_w/M_n = 1.11.

Synthesis mPEG-*b*-(εCL-*co*-2) (5). According to the general procedure described above, mPEG (500 mg, 0.25 mmol, 1 equiv) was dried and dissolved in dichloromethane. Dry ε-caprolactone (83 μL, 0.75 mmol, 3 equiv) and **2** (134.4 μL, 1 mmol, 4 equiv) were introduced, and the polymerization started by the addition of HCl in ether (0.75 mL, 0.75 mmol, 3 equiv). After 24 h, the polymer was precipitated twice in cold *n*-hexane to yield **5** as a white solid. The fully annotated NMR spectrum can be found in Supporting Information Figure S4. This polymer contains on average four units of **2** per polymer chain. SEC (DMF): M_n = 2000 g/mol, M_w/M_n = 1.18.

NC Preparation. PTX NCs were produced by wet milling. In a typical experiment, 2 mL of a 5% (w/w) polymer solution in ultrapure water was filtered (0.2 μm pore size) into a 20 mL cylindrical glass vessel containing 10 mg of PTX and 4 mL of zirconium oxide beads (~14.7 g, 0.3 mm in diameter, Union Process, Akron, OH). The vessel was sealed with a plastic cap and then placed horizontally on a Ratek BTR5 blood tube roller (with custom modified motor, Labortechnik Fröbel GmbH, Lindau, Germany) and rolled at 220 rpm for 48 h in a cold room (6 °C). After milling, the beads were separated from the suspension by filtration through polyamide sieve fabric (30 μm pores, VWR, Dietikon, Switzerland), and the residue was washed four times with 2 mL of ultrapure water. The suspension was centrifuged at 12000*g* for 6 min to remove larger aggregates. The supernatant was then subjected to SEC with Sepharose CL-4B to remove excess polymer, typically yielding a suspension containing 0.55 or 0.74 mg/mL PTX for polymers **3** or **4**, respectively.

Cross-Linking in Solution. In a proof of principle experiment, a 1.8 mM solution of **3** was reacted with **7** at two different ratios (1/1 and 1/10 azide/alkyne) in a solution containing 1.8 mM copper sulfate and 9 mM sodium ascorbate for 20 min. The reaction mixture was then frozen in liquid nitrogen, lyophilized, and dissolved in $CDCl_3$ for ^{1}H NMR analysis and subsequent FTIR analysis.

Cross-Linking on NCs. For cross-linking in the presence of NCs, the procedure above was slightly modified. As a general example, **7** (0.159 mg, 0.65 μmol, 2.5/1 molar equiv azide/alkyne) in ethanol was transferred to a round-bottom flask and the solvent removed under a stream of nitrogen. Then, 3 mL of NC suspension (~0.55 mg/mL PTX, ~0.262 μmol alkyne) was added followed by 10 μL of a solution containing 100 mM sodium ascorbate and 20 mM copper sulfate, with final concentrations of 333 and 67 μM, respectively. Owing to the different solubility characteristics of **5** and **6**, they were dissolved in water and NMP, respectively, and added after the catalyst. The flask was placed on a rotary shaker (~100 rpm) at room temperature for 24 h. After this period, the cross-linked NCs were separated from catalyst and excess cross-linker by SEC using Sephadex G10. The fraction with the highest concentration (~0.5 mg/mL PTX) was used for measuring particle size with time by DLS at both 6 and 20 °C. For ^{1}H NMR and FTIR analyses, the fractions were pooled, frozen in liquid nitrogen, and lyophilized to concentrate the NCs. Then, deuterated methanol was added to the lyophilized powder, which was then sonicated at 45 °C to form a homogeneous suspension that was then analyzed. A summary of all cross-linking conditions examined herein is given in Table 1.

Imaging of NCs and the Polymer Coating after PTX Removal. For transmission electron microscopy (TEM), samples (4 μL) of the NC suspension, prepared at a concentration of ~0.5 mg/mL PTX, were adsorbed to glow discharged carbon-coated copper grids for 1 min. After two washings with water to remove excess NCs, they were negatively stained with 2% (w/v) uranyl acetate for 1 min and air-dried after blotting with filter paper. The specimens were examined in a Philips CM12 (tungsten cathode) transmission electron microscope (FEI, Hillsboro, OR) at 100 kV, and images were recorded with a Gatan CCD 794 camera (Gatan Inc., Pleasanton, CA).

To dissolve the drug within nanocages, the NCs (3 mL in water, ~0.5 mg/mL) were added to a 5 mL Spectra/Por Float-A-Lyzer G2 (MWCO 100 kDa, Sigma-Aldrich, Buchs, Switzerland) and, after addition of 870 μL of ethanol, were dialyzed against 2.5 L 25% ethanol/water mixture. The drug concentration inside the dialysis bag was measured before medium change every day by HPLC. After complete removal of drug, the contents inside the dialysis bag were concentrated with Spectra/Gel Absorbent (VWR, International AG, Dietikon, Switzerland) to about 0.5 mL (~0.4 mg/mL of polymer) and analyzed by TEM. The presence of mPEG was tested by adding CoSCN to the concentrate.[54] Samples were prepared according to the protocol for NC suspension, but without the extra washing steps.

Particle Volume and Polymer Coverage Calculations. From TEM images, the average dimensions of the NCs were measured (n = 138). Using eq 1, the number of polymer chains ($n_{Polymer}$) per NC could be calculated

$$n_{Polymer} = N_A V \rho (wt_{Polymer}/wt_{PTX})/M_{wPolymer} \quad (1)$$

where N_A is Avogadro's constant, V is the average volume of a NC (assumed to be a cylinder), ρ is the density (1.4035 g/mL for PTX dihydrate), ($wt_{Polymer}/wt_{PTX}$) is the weight ratio of drug to polymer after purification determined by ^{1}H NMR spectroscopy, and M_w is the weight average molecular weight of the polymer.

Dissolution Test. Release of PTX from NCs was tested under sink conditions in 5% BSA solution, which is expected to be the main solubilizing component for PTX *in vivo*.[55] In a preliminary experiment, the saturation solubility of PTX powder in the test conditions was found to be 0.01 mg/mL. A 1 mL Spectra/Por Float-A-Lyzer G2 (MWCO 100 kDa, Sigma-Aldrich, Buchs, Switzerland) was filled by mixing 20 mM phosphate buffer (pH 7.4) containing 10% BSA with NCs in water to yield a final volume of 1 mL containing 0.1 mg/mL PTX in 10 mM phosphate buffer (pH 7.4) and 5% BSA. The dialysis device was placed in a 50 mL centrifugation tube containing 45 mL of 10 mM phosphate buffer (pH 7.4) with 5% BSA, on a rotary shaker (~400 rpm) in an incubator at 37 °C. Under these conditions, the maximum PTX concentration was 5 times below its saturation solubility. At selected time points, 30 μL aliquots were taken from inside the dialysis device and prepared for HPLC analysis by addition of 60 μL of internal standard and 100 μL of methanol. The samples were stored at −20 °C overnight to precipitate albumin. The precipitate was removed by centrifugation, and the supernatant was filtered through polyamide (0.2 μm pore size) and analyzed.

Polymer Shedding Test. Dispersions of NCs with either non-cross-linked or cross-linked coatings (**4** cross-linked with **7**) were diluted to a PTX concentration of 0.4 mg/mL in water. The dispersions were then repeatedly centrifuged at 20 000*g* for 45 min at 14 °C until the supernatant contained a stable concentration of PTX (measured by UV−vis spectroscopy at 230 nm). This procedure lead to removal of ~95% of the initially present PTX. The supernatant was lyophilized and residual mPEG content was analyzed by ^{1}H NMR spectroscopy in D_2O using DMSO as internal standard for quantitative analysis.

Statistical Analysis. Differences in groups were calculated by one-way ANOVA (normal distribution was assumed) followed by a Tukey *post hoc* test. A value of $p < 0.05$ was considered significant.

Equipment. ^{1}H NMR spectra were recorded on a Bruker Av400 spectrometer (Bruker BioSpin, Fällanden, Switzerland) operating at 400 MHz for protons. Analytical size-exclusion chromatography (SEC) measurements were performed in 0.01 M LiBr in DMF using a Viscotek TDAmax system (Viscotek, Houston, TX) equipped with a differential refractive index detector. Molecular weights are given relative to narrow PEG standards (PSS Polymer Standards Service GmbH, Mainz,

Germany). Separation was achieved using two Viscotek columns (CLM 3047) in series at a flow rate of 1.0 mL/min at 45 °C. Particle hydrodynamic diameter was determined by dynamic light scattering (DLS) using a DelsaNano C particle analyzer (Beckman Coulter, Brea, CA). The cumulants result calculated by the software was used to report the hydrodynamic diameter of the NCs. PTX concentration was determined by HPLC analysis, using an autosampler and pump system (CTC, Thermo Fisher) equipped with a reversed phase column (Hypersil Gold column, 1 × 100 mm, Thermo Fisher) heated to 30 °C (HotDog column oven) and an Accela PDA detector (Thermo Fisher Scientific, Reinach, Switzerland). Gradient elution was performed starting with a mix of 55% methanol in water (both containing 0.1% formic acid) rising to 85% methanol within 15 min. PTX was detected at 227 nm. A solution of docetaxel in methanol was added as internal standard. FTIR spectra were obtained using ATR geometry on a Spectrum 65 infrared spectrophotometer (Perkin-Elmer, Schwerzenbach, Switzerland). After centrifugation of NC dispersions (180 min, at 19 000*g*), the copper concentration in the supernatant was measured by ICP-OES relative to aqueous $CuSO_4$ standards (ULTIMA 2 ICP-OES, HORIBA Jobin Yvon Gmbh, Unterhaching, Germany).

Conflict of Interest: The authors declare no competing financial interest.

Acknowledgment. The authors acknowledge A. E. Felber for the acquisition of TEM images supported by the Electron Microscopy Center of ETH Zurich (EMEZ), and M. Rossier (Functional Materials Laboratory, Institute for Chemical and Bioengineering, ETH) for ICP-OES measurements.

Supporting Information Available: Supplementary synthetic protocols, characterization of compounds (NMR and FTIR spectra), optimization of milling experiments, cross-linking in solution, and supplementary stability and dissolution experiments are provided. This material is available free of charge *via* the Internet at http://pubs.acs.org.

REFERENCES AND NOTES

1. Aggarwal, P.; Hall, J. B.; McLeland, C. B.; Dobrovolskaia, M. A.; McNeil, S. E. Nanoparticle Interaction with Plasma Proteins as It Relates to Particle Biodistribution, Biocompatibility and Therapeutic Efficacy. *Adv. Drug Delivery Rev.* **2009**, *61*, 428–437.
2. Lipinski, C. A. Drug-like Properties and the Causes of Poor Solubility and Poor Permeability. *J. Pharmacol. Toxicol. Methods* **2000**, *44*, 235–249.
3. Lindfors, L.; Forssen, S.; Skantze, P.; Skantze, U.; Zackrisson, A.; Olsson, U. Amorphous Drug Nanosuspensions. 2. Experimental Determination of Bulk Monomer Concentrations. *Langmuir* **2005**, *22*, 911–916.
4. Meerum Terwogt, J. M.; Nuijen, B.; Ten Bokkel Huinink, W. W.; Beijnen, J. H. Alternative Formulations of Paclitaxel. *Cancer Treat. Rev.* **1997**, *23*, 87–95.
5. Gelderblom, H.; Verweij, J.; Nooter, K.; Sparreboom, A. Cremophor EL: The Drawbacks and Advantages of Vehicle Selection for Drug Formulation. *Eur. J. Cancer* **2001**, *37*, 1590–1598.
6. Fahr, A.; Liu, X. Drug Delivery Strategies for Poorly Water-Soluble Drugs. *Expert Opin. Drug Delivery* **2007**, *4*, 403–416.
7. Chan, J. M.; Zhang, L.; Tong, R.; Ghosh, D.; Gao, W.; Liao, G.; Yuet, K. P.; Gray, D.; Rhee, J.-W.; Cheng, J.; *et al.* Spatiotemporal Controlled Delivery of Nanoparticles to Injured Vasculature. *Proc. Natl. Acad. Sci. U.S.A.* **2010**, *107*, 2213–2218.
8. Hayashi, Y.; Skwarczynski, M.; Hamada, Y.; Sohma, Y.; Kimura, T.; Kiso, Y. A Novel Approach of Water-Soluble Paclitaxel Prodrug with No Auxiliary and No Byproduct: Design and Synthesis of Isotaxel. *J. Med. Chem.* **2003**, *46*, 3782–3784.
9. Van, S.; Das, S. K.; Wang, X.; Feng, Z.; Jin, Y.; Hou, Z.; Chen, F.; Pham, A.; Jiang, N.; Howell, S. B.; *et al.* Synthesis, Characterization, and Biological Evaluation of Poly(L-γ-glutamyl-glutamine)-Paclitaxel Nanoconjugate. *Int. J. Nanomed.* **2010**, *5*, 825–837.
10. Dosio, F.; Reddy, L. H.; Ferrero, A.; Stella, B.; Cattel, L.; Couvreur, P. Novel Nanoassemblies Composed of Squalenoyl−Paclitaxel Derivatives: Synthesis, Characterization, and Biological Evaluation. *Bioconjugate Chem.* **2010**, *21*, 1349–1361.
11. Zhang, J. A.; Anyarambhatla, G.; Ma, L.; Ugwu, S.; Xuan, T.; Sardone, T.; Ahmad, I. Development and Characterization of a Novel Cremophor® EL Free Liposome-Based Paclitaxel (LEP-ETU) Formulation. *Eur. J. Pharm. Biopharm.* **2005**, *59*, 177–187.
12. Liu, Z.; Chen, K.; Davis, C.; Sherlock, S.; Cao, Q.; Chen, X.; Dai, H. Drug Delivery with Carbon Nanotubes for *In Vivo* Cancer Treatment. *Cancer Res.* **2008**, *68*, 6652–6660.
13. Brewster, M. E.; Loftsson, T. Cyclodextrins as Pharmaceutical Solubilizers. *Adv. Drug Delivery Rev.* **2007**, *59*, 645–666.
14. Le Garrec, D.; Gori, S.; Luo, L.; Lessard, D.; Smith, D. C.; Yessine, M. A.; Ranger, M.; Leroux, J. C. Poly(*N*-vinylpyrrolidone)-Block-Poly(D,L-lactide) as a New Polymeric Solubilizer for Hydrophobic Anticancer Drugs: *In Vitro* and *In Vivo* Evaluation. *J. Controlled Release* **2004**, *99*, 83–101.
15. Gardner, E. R.; Dahut, W. L.; Scripture, C. D.; Jones, J.; Aragon-Ching, J. B.; Desai, N.; Hawkins, M. J.; Sparreboom, A.; Figg, W. D. Randomized Crossover Pharmacokinetic Study of Solvent-Based Paclitaxel and *nab*-Paclitaxel. *Clin. Cancer Res.* **2008**, *14*, 4200–4205.
16. Li, C.; Wallace, S. Polymer-Drug Conjugates: Recent Development in Clinical Oncology. *Adv. Drug Delivery Rev.* **2008**, *60*, 886–898.
17. Kogan, A.; Garti, N. Microemulsions as Transdermal Drug Delivery Vehicles. *Adv. Colloid Interface Sci.* **2006**, *123−126*, 369–385.
18. Strickley, R. Solubilizing Excipients in Oral and Injectable Formulations. *Pharm. Res.* **2004**, *21*, 201–230.
19. Chiappetta, D. A.; Sosnik, A. Poly(ethylene oxide)-Poly(propylene oxide) Block Copolymer Micelles as Drug Delivery Agents: Improved Hydrosolubility, Stability and Bioavailability of Drugs. *Eur. J. Pharm. Biopharm.* **2007**, *66*, 303–317.
20. Soussan, E.; Cassel, S.; Blanzat, M.; Rico-Lattes, I. Drug Delivery by Soft Matter: Matrix and Vesicular Carriers. *Angew. Chem., Int. Ed.* **2009**, *48*, 274–288.
21. Serajuddin, A. T. M. Solid Dispersion of Poorly Water-Soluble Drugs: Early Promises, Subsequent Problems, and Recent Breakthroughs. *J. Pharm. Sci.* **1999**, *88*, 1058–1066.
22. Sylvestre, J.-P.; Tang, M.-C.; Furtos, A.; Leclair, G.; Meunier, M.; Leroux, J.-C. Nanonization of Megestrol Acetate by Laser Fragmentation in Aqueous Milieu. *J. Controlled Release* **2011**, *149*, 273–280.
23. Date, A. A.; Patravale, V. B. Current Strategies for Engineering Drug Nanoparticles. *Curr. Opin. Colloid Interface Sci.* **2004**, *9*, 222–235.
24. Merisko-Liversidge, E. M.; Liversidge, G. G. Drug Nanoparticles: Formulating Poorly Water-Soluble Compounds. *Toxicol. Pathol.* **2008**, *36*, 43–48.
25. Rabinow, B. E. Nanosuspensions in Drug Delivery. *Nat. Rev. Drug Discovery* **2004**, *3*, 785–796.
26. Merisko-Liversidge, E.; Liversidge, G. G.; Cooper, E. R. Nanosizing: A Formulation Approach for Poorly-Water-Soluble Compounds. *Eur. J. Pharm. Sci.* **2003**, *18*, 113–120.
27. Van Eerdenbrugh, B.; Van den Mooter, G.; Augustijns, P. Top-Down Production of Drug Nanocrystals: Nanosuspension Stabilization, Miniaturization and Transformation into Solid Products. *Int. J. Pharm.* **2008**, *364*, 64–75.
28. Liu, F.; Park, J.-Y.; Zhang, Y.; Conwell, C.; Liu, Y.; Bathula, S. R.; Huang, L. Targeted Cancer Therapy with Novel High Drug-Loading Nanocrystals. *J. Pharm. Sci.* **2010**, *99*, 3542–3551.
29. Liu, Y.; Huang, L.; Liu, F. Paclitaxel Nanocrystals for Overcoming Multidrug Resistance in Cancer. *Mol. Pharmaceutics* **2010**, *7*, 863–869.
30. Wu, L.; Zhang, J.; Watanabe, W. Physical and Chemical Stability of Drug Nanoparticles. *Adv. Drug Delivery Rev.* **2011**, *63*, 456–469.

31. Agarwal, A.; Lvov, Y.; Sawant, R.; Torchilin, V. Stable Nanocolloids of Poorly Soluble Drugs with High Drug Content Prepared Using the Combination of Sonication and Layer-by-Layer Technology. *J. Controlled Release* **2008**, *128*, 255–260.
32. Ibrahim, N. K.; Desai, N.; Legha, S.; Soon-Shiong, P.; Theriault, R. L.; Rivera, E.; Esmaeli, B.; Ring, S. E.; Bedikian, A.; Hortobagyi, G. N.; *et al.* Phase I and Pharmacokinetic Study of ABI-007, a Cremophor-Free, Protein-Stabilized, Nanoparticle Formulation of Paclitaxel. *Clin. Cancer Res.* **2002**, *8*, 1038–1044.
33. Sugahara, K. N.; Teesalu, T.; Karmali, P. P.; Kotamraju, V. R.; Agemy, L.; Greenwald, D. R.; Ruoslahti, E. Coadministration of a Tumor-Penetrating Peptide Enhances the Efficacy of Cancer Drugs. *Science* **2010**, *328*, 1031–1035.
34. Karmali, P. P.; Kotamraju, V. R.; Kastantin, M.; Black, M.; Missirlis, D.; Tirrell, M.; Ruoslahti, E. Targeting of Albumin-Embedded Paclitaxel Nanoparticles to Tumors. *Nanomedicine* **2009**, *5*, 73–82.
35. Deng, J.; Huang, L.; Liu, F. Understanding the Structure and Stability of Paclitaxel Nanocrystals. *Int. J. Pharm.* **2010**, *390*, 242–249.
36. Turner, J. L.; Chen, Z.; Wooley, K. L. Regiochemical Functionalization of a Nanoscale Cage-like Structure: Robust Core−Shell Nanostructures Crafted as Vessels for Selective Uptake and Release of Small and Large Guests. *J. Controlled Release* **2005**, *109*, 189–202.
37. Alexis, F.; Pridgen, E.; Molnar, L. K.; Farokhzad, O. C. Factors Affecting the Clearance and Biodistribution of Polymeric Nanoparticles. *Mol. Pharmaceutics* **2008**, *5*, 505–515.
38. Torchilin, V. P. Multifunctional Nanocarriers. *Adv. Drug Delivery Rev.* **2006**, *58*, 1532–1555.
39. Ahmed, F.; Discher, D. E. Self-Porating Polymersomes of PEG-PLA and PEG-PCL: Hydrolysis-Triggered Controlled Release Vesicles. *J. Controlled Release* **2004**, *96*, 37–53.
40. Kim, M. S.; Seo, K. S.; Khang, G.; Lee, H. B. Ring-Opening Polymerization of ε-Caprolactone by Poly(ethylene glycol) by an Activated Monomer Mechanism. *Macromol. Rapid Commun.* **2005**, *26*, 643–648.
41. Parrish, B.; Breitenkamp, R. B.; Emrick, T. PEG- and Peptide-Grafted Aliphatic Polyesters by Click Chemistry. *J. Am. Chem. Soc.* **2005**, *127*, 7404–7410.
42. Riva, R.; Schmeits, S.; Stoffelbach, F.; Jerome, C.; Jerome, R.; Lecomte, P. Combination of Ring-Opening Polymerization and "Click" Chemistry towards Functionalization of Aliphatic Polyesters. *Chem. Commun.* **2005**, 5334–5336.
43. Merisko-Liversidge, E.; Sarpotdar, P.; Bruno, J.; Hajj, S.; Wei, L.; Peltier, N.; Rake, J.; Shaw, J. M.; Pugh, S.; Polin, L.; *et al.* Formulation and Antitumor Activity Evaluation of Nanocrystalline Suspensions of Poorly Soluble Anticancer Drugs. *Pharm. Res.* **1996**, *13*, 272–278.
44. Cerdeira, A. M.; Mazzotti, M.; Gander, B. Miconazole Nanosuspensions: Influence of Formulation Variables on Particle Size Reduction and Physical Stability. *Int. J. Pharm.* **2010**, *396*, 210–218.
45. Van Eerdenbrugh, B.; Vermant, J.; Martens, J. A.; Froyen, L.; Humbeeck, J. V.; Van den Mooter, G.; Augustijns, P. Solubility Increases Associated with Crystalline Drug Nanoparticles: Methodologies and Significance. *Mol. Pharmaceutics* **2010**, *7*, 1858–1870.
46. Budijono, S. J.; Russ, B.; Saad, W.; Adamson, D. H.; Prud'homme, R. K. Block Copolymer Surface Coverage on Nanoparticles. *Colloids Surf., A* **2010**, *360*, 105–110.
47. Pasche, S.; De Paul, S. M.; Vörös, J.; Spencer, N. D.; Textor, M. Poly(L-lysine)-Graft-Poly(ethylene glycol) Assembled Monolayers on Niobium Oxide Surfaces: A Quantitative Study of the Influence of Polymer Interfacial Architecture on Resistance to Protein Adsorption by ToF-SIMS and *In Situ* OWLS. *Langmuir* **2003**, *19*, 9216–9225.
48. Turner, J. L.; Wooley, K. L. Nanoscale Cage-like Structures Derived from Polyisoprene-Containing Shell Cross-Linked Nanoparticle Templates. *Nano Lett.* **2004**, *4*, 683–688.
49. Horn, D.; Rieger, J. Organic Nanoparticles in the Aqueous Phase—Theory, Experiment, and Use. *Angew. Chem., Int. Ed.* **2001**, *40*, 4330–4361.
50. Lindfors, L.; Skantze, P.; Skantze, U.; Rasmusson, M.; Zackrisson, A.; Olsson, U. Amorphous Drug Nanosuspensions. 1. Inhibition of Ostwald Ripening. *Langmuir* **2005**, *22*, 906–910.
51. Zhao, R.; Hollis, C. P.; Zhang, H.; Sun, L.; Gemeinhart, R. A.; Li, T. Hybrid Nanocrystals: Achieving Concurrent Therapeutic and Bioimaging Functionalities toward Solid Tumors. *Mol. Pharmaceutics* **2011**, *8*, 1985–1991.
52. Venkataraman, S.; Hedrick, J. L.; Ong, Z. Y.; Yang, C.; Ee, P. L. R.; Hammond, P. T.; Yang, Y. Y. The Effects of Polymeric Nanostructure Shape on Drug Delivery. *Adv. Drug Delivery Rev.* **2011**, *63*, 1228–1246.
53. Lenoir, S.; Riva, R.; Lou, X.; Detrembleur, C.; Jérôme, R.; Lecomte, P. Ring-Opening Polymerization of α-Chloro-ε-caprolactone and Chemical Modification of Poly(α-chloro-ε-caprolactone) by Atom Transfer Radical Processes. *Macromolecules* **2004**, *37*, 4055–4061.
54. Ghebeh, H.; Handa-Corrigan, A.; Butler, M. Development of an Assay for the Measurement of the Surfactant Pluronic F-68 in Mammalian Cell Culture Medium. *Anal. Biochem.* **1998**, *262*, 39–44.
55. Letchford, K.; Liggins, R.; Wasan, K. M.; Burt, H. *In Vitro* Human Plasma Distribution of Nanoparticulate Paclitaxel Is Dependent on the Physicochemical Properties of Poly(ethylene glycol)-Block-Poly(caprolactone) Nanoparticles. *Eur. J. Pharm. Biopharm.* **2009**, *71*, 196–206.